Journal of Vacuum Science and Technology B

RESEARCH ARTICLE | OCTOBER 14 2024

Rubbing-induced site-selective deposition of 2D material patterns on nanomembranes

Special Collection: Papers from the 67th International Conference on Electron, Ion and Photon Beam Technology and Nanofabrication (EIPBN 2024)

Mingze Chen ; Xiaoqiu An; Seungjun Ki ; Xiaogan Liang

J. Vac. Sci. Technol. B 42, 062801 (2024)
https://doi.org/10.1116/6.0003961

JVST B
Journal of Vacuum Science & Technology B

ARTICLE

pubs.aip.org/avs/jvb

Rubbing-induced site-selective deposition of 2D material patterns on nanomembranes

Cite as: J. Vac. Sci. Technol. B **42**, 062801 (2024); doi: 10.1116/6.0003961
Submitted: 6 August 2024 · Accepted: 30 September 2024 ·
Published Online: 14 October 2024

Mingze Chen, Xiaoqiu An, Seungjun Ki, and Xiaogan Liang[a)]

AFFILIATIONS

Mechanical Engineering Department, University of Michigan, Ann Arbor, Michigan 48109

Note: This paper is part of the Special Topic Collection: Papers from the 67th International Conference on Electron, Ion and Photon Beam Technology and Nanofabrication (EIPBN 2024).

[a)]**Electronic mail:** xiaoganl@umich.edu

ABSTRACT

2D-layered materials (e.g., graphene and transition metal dichalcogenides) have attracted huge attention due to their unique mechanical and electrical properties. Emerging research efforts, which seek to combine device characterization and high-resolution electron micrography analysis for 2D-layered device features, demand nano/microlithographic techniques capable of producing ordered 2D material patterns on ultrathin membranes with nanoscale thicknesses. However, such membranes are so fragile that most conventional lithographic techniques can be hardly performed on them to generate 2D material patterns. Our previous works have demonstrated that the rubbing-induced site-selective (RISS) deposition method can produce arbitrary 2D semiconductor (e.g., MoS_2 and Bi_2Se_3) patterns on regular device substrates. This fabrication route prevents the vulnerable 2D-layered structures from the detrimental damage introduced by plasma etching and resist-based lithography processes. In this work, we explore the applicability of RISS for directly producing 2D material patterns on nanomembranes. Specifically, this work shows that a polymeric interfacing layer on the rubbing template features, which can effectively prevent stress concentration during the rubbing process, is crucial to successful implementation of RISS processes on nanomembranes. Furthermore, we carried out the mechanics simulation of the Von Mises stress and pressure distribution on the RISS-processed membrane to identify the optimal rubbing load, which can generate sufficient triboelectric charge for material deposition but no damage to the membrane. Using this approach, we have successfully demonstrated the deposition of Bi_2Se_3 patterns on 25 nm SiO_x nanomembranes and high-resolution transmission electron micrography characterization of the crystallographic structures.

I. INTRODUCTION

2D-layered materials, such as graphene, molybdenum disulfide (MoS_2), and hexagonal boron nitride (h-BN), have been exploited to make novel electronics and optoelectronic devices of various sorts.[1–6] Their unique layered structure endows them with high sensitivity to the external stimulus, which makes them the ideal candidates for making sensing devices. However, during the fabrication of nano- and microscale devices based on such 2D materials, resist-based lithography and plasma etching processes are inevitably performed on such fragile 2D-layered materials and result in permanent contaminations and damages.[7,8] Current standard cleaning methods (e.g., piranha cleaning) also introduce unwanted chemical or mechanical damages to 2D device features, which could compromise the performance of the devices and increase the device-to-device variations. Our previously published works report a rubbing-induced site-selective (RISS) deposition method, which is capable of producing arbitrary MoS_2 and Bi_2Se_3 features on regular SiO_2/Si substrates without additional etching and lithography processes.[9–11] The RISS process leverages the rubbing-induced triboelectric charge pattern as the preferable nucleation sites for the deposition precursors of the 2D materials, therefore realizing site-selective deposition of well-defined 2D material patterns. Specifically, the nonuniform electrical field radiated from the triboelectric charge patterns polarizes the vaporized molecular compounds (or precursor molecules) of the target 2D material, which are attracted and nucleated within the charged areas due to the dipole interaction. This deposition method can fabricate arrays of 2D material patterns on regular SiO_2/Si substrates with a high yield and uniformity.[10] The RISS-produced MoS_2 features have been also found to have prominent photon-sensitive and memristive characteristics, suitable for photodetection and memristive device

applications.[12–14] In addition, we have also utilized the RISS-produced Bi_2Se_3 memristors to realize a hardware-based neuromorphic system for processing analog video signals.[11] Recently, many emerging research efforts about 2D materials and devices seek to simultaneously examine the dynamic evolution of the atomic structures of 2D materials and the transport characteristics of the devices made from such 2D materials. Such research missions demand nano- or microlithographic techniques capable of producing orderly arranged or addressable 2D-material-based device patterns on ultrathin membranes with nanoscale thicknesses, aiming to enable *in situ* high-resolution transmission electron microscopy (HRTEM) characterization of such 2D device features during the device operation.[15,16] However, such nanoscale thick membranes are so fragile that most conventional lithographic techniques can be hardly performed on them to generate 2D material patterns. Such a generic need motivates us to investigate the applicability of RISS processes on ultrathin nanomembranes. Specifically, because the current rubbing scheme of RISS could generate irreversible mechanical damages on nanomembranes, additional experimental and simulation works are needed to address this technical challenge. Specifically, a quantitative analysis on applied rubbing load and the morphology of the rubbing template is necessary for the successful implementation of RISS processes on fragile nanomembranes. Such a technical capability is highly demanded by emerging research tasks seeking to directly observe and understand the dynamic evolution of the crystalline structures of 2D devices during the device operations. Furthermore, if RISS enables 2D device fabrication on nanomembranes, its application scope could be further leveraged for producing new flexible electronic and optoelectronic devices as well as developing new packaging, transfer-printing, and device integration techniques.

In this article, we report our recent progress in the site-selective deposition of layered Bi_2Se_3 patterns on nanomembranes using the RISS deposition process. To avoid the mechanical damage caused by the rubbing process, we introduce a polymeric interfacing layer on the rubbing template features to uniformly distribute the mechanical load and prevent excessive stress concentration on the nanomembranes. Finite element analysis (FEA) simulations are also performed under different load conditions for two types of rubbing features, which theoretically confirms the experimental results. Using such an experimental/theoretical-integrated method, we also identified the appropriate rubbing load, which can generate sufficient triboelectric charge density (and electric potential) for site-selective deposition but does not damage the substrate. Finally, using 20 μm diameter rubbing pillars with polymeric interfacing layers under mechanical load of 0.4 N, we can successfully deposit Bi_2Se_3 patterns on the nanomembranes for HRTEM analysis. The obtained HRTEM micrographs and fast Fourier transform (FFT) analysis results show that the RISS-produced Bi_2Se_3 films have a hexagonal, single-crystal structure. This research provides a method to directly deposit 2D-layered materials on nanomembranes, which can enable *in situ* HRTEM and other relevant characterizations for 2D material-based devices.

II. EXPERIMENTS

A. Nanomembrane samples and rubbing processes

Figure 1(a) shows the optical microscope (OM) image of an as-received nanomembrane sample (Norcada Inc.) for HRTEM characterization, which has twenty-four 40 μm diameter, 25 nm thick SiO_2 nanomembrane regions on a 0.4 × 0.4 mm size, 500 nm thick SiN_xO_y support film, as well as a 300 μm thick Si frame. Figure 1(b) illustrates the cross-sectional view of the whole nanomembrane sample. Figures 1(c)–1(e) schematically illustrate the fabrication process of the patterned Bi_2Se_3 features on the SiO_2 nanomembranes using the rubbing-induced site-selective deposition (RISS) process. Because the HRTEM sample is relatively small and fragile, an adhesion layer is applied to mount the Si frame on a glass carrier substrate. In a rubbing process, the rubbing template bearing Au-coated protrusive pillars is aligned with the HRTEM sample by using a lab-built moving stage system. Afterward, the HRTEM sample is elevated by the Z-stage to contact with the rubbing template [Fig. 1(c)]. The protrusive pillars on the rubbing template rub on the nanomembranes with the preset load and trajectory to generate triboelectric charge patterns on the nanomembranes[17,18] [Fig. 1(d)]. Here, the applied load is constantly monitored by a force gauge mounted on the top of the rubbing template, and the rubbing trajectory is controlled by the x–y stages. After the rubbing process, the nanomembrane sample with triboelectric charge patterns is loaded into a deposition furnace for Bi_2Se_3 deposition [Fig. 1(e)]. A more detailed description of the rubbing process is presented in our previous work.[10]

B. Rubbing template fabrication and modification

A photoresist (SPR220) film is spin-coated on a 300 nm SiO_2/500 μm Si substrate and soft-baked at 115 °C for 90 s. Afterward, on a photoaligner (MJB3-2), this substrate coated with photoresist is aligned with a photomask bearing a 24 × 24 array of square patterns with a feature size of 10 μm and period of 80 μm, followed by UV exposure. After the developing process, the SiO_2 layer on the substrate is etched through by using a glass etcher (STS APS DGRIE) to form SiO_2 mask features. Subsequently, reactive ion etching (RIE) of Si is performed by using a STS Pegasus tool to etch the revealed silicon on the substrate with the SiO_2 features as the etching masks. This etching process forms 40 μm high protrusive pillar arrays dedicated to the rubbing processes. In this work, two types of rubbing pillars are tested for rubbing nanomembranes: (1) nanostrip-cleaned pillars and (2) photoresist-coated pillars. To make the first type of pillars, after the etching process, the pillar array is soaked in a nanostrip for 20 min to fully remove the photoresist film. Figure 2(a) shows the tilted-view SEM image of such a fully cleaned pillar. To make the second type of pillars, a polymeric interfacing layer is introduced by coating the cleaned pillars with additional 3 μm thick photoresist followed with a brief O_2 plasma treatment that results in a crosslinked polymer coating film, as shown in Fig 2(b). Such an interfacing layer serves as a cushion between the rubbing pillars and the substrate to avoid excessive stress concentration, which is the key factor for inducing fracture in solid films. Finally, for both types of rubbing pillars, 10 nm Ti followed by 100 nm Au is coated on the fabricated pillars as the rubbing layer for generating a high triboelectric charge density.[10]

C. Bi_2Se_3 deposition process

After the rubbing process, the rubbed nanomembrane sample with triboelectric charge patterns is loaded into a vacuum furnace

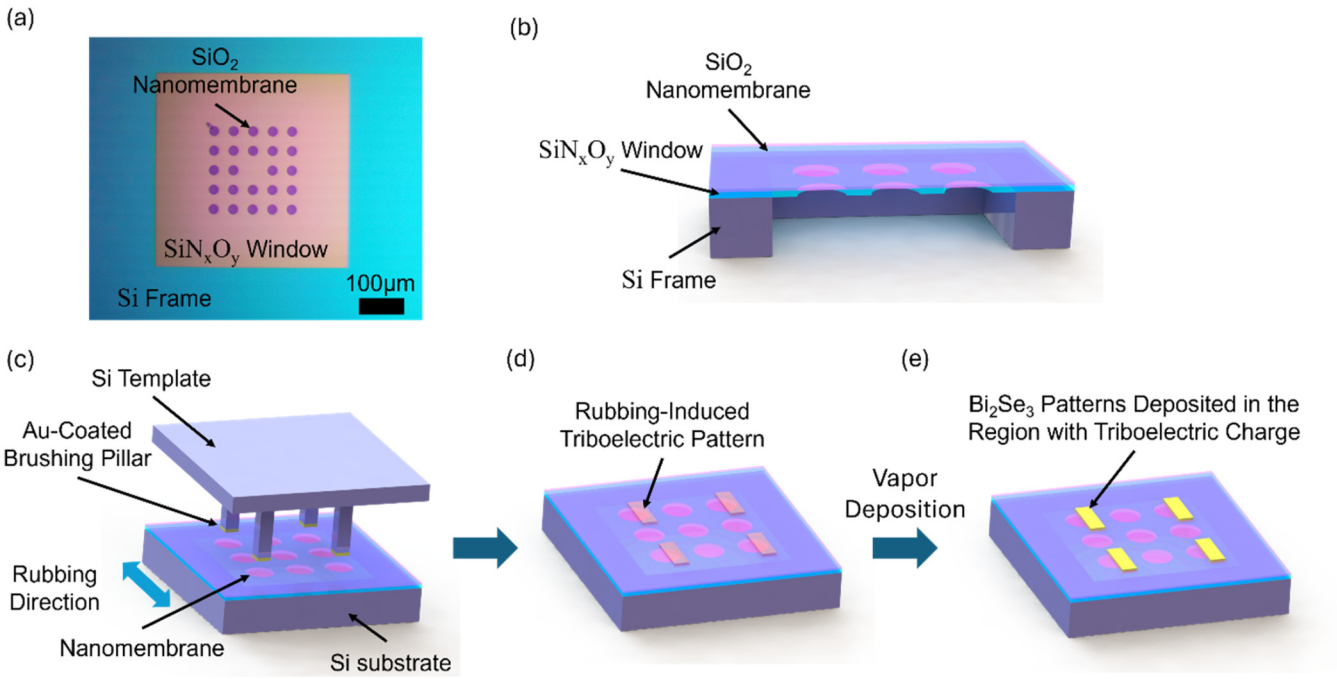

FIG. 1. (a) Optical microscope image of an as-received nanomembrane sample for HRTEM characterization; (b) cross-sectional illustration of the nanomembrane sample. (c)–(e) Schematic flow chart of the fabrication process of the patterned Bi_2Se_3 features on SiO_2 nanomembranes using the rubbing-induced site-selective deposition (RISS) process: (c) A Si rubbing template bearing Au-coated brushing pillars is brought into contact with the nanomembrane sample; (d) the protrusive brushing pillars are actuated by moving stages and rub on the nanomembranes with the preset load and trajectory to generate triboelectric charge patterns on the nanomembranes; (e) Bi_2Se_3 patterns are selectively deposited within the rubbed areas on the circular nanomembrane areas after the vapor deposition process.

for Bi_2Se_3 deposition. Specifically, 10 mg of bismuth selenide powder (Bi_2Se_3, 99.995%, Sigma-Aldrich) is placed in an alumina crucible (AdValue Technology) located at the center of the furnace. The nanomembrane sample with triboelectric charge patterns is placed facing up at a downstream location of the furnace. The system is pumped to 100 mTor and purged with argon gas (99.999%, cryogenic gases) at the flow rate of 180 SCCM for 15 min to remove any pollution from air. The argon, serving as the carrier gas, constantly flows into the system throughout the entire deposition process at the flow rate of 80 SCCM. The furnace is heated to 550 °C and maintained for 7 min for Bi_2Se_3 deposition. During a deposition process, the Bi_2Se_3 powder is vaporized in the furnace and recondensed on the nanomembrane that is placed in the region at 350 °C. Afterward, the furnace is turned off, and it naturally cools down to the room temperature.

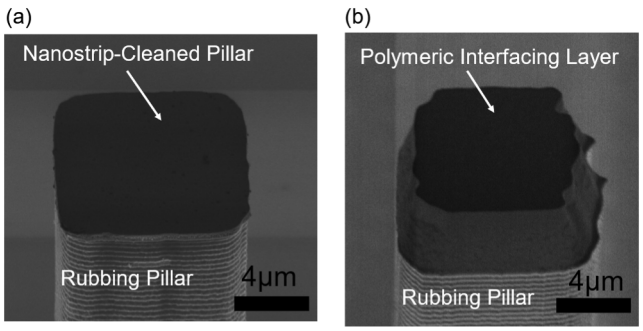

FIG. 2. Tilted-view SEM images of rubbing pillars: (a) fully cleaned rubbing pillar; (b) rubbing pillar with a polymeric interfacing layer.

III. RESULTS AND DISCUSSION

The main goal of this work is to identify the appropriate RISS processing conditions capable of generating well-defined 2D material features on 25 nm thick SiO_2 membranes without inducing mechanical damage to the membranes. The key technical concern is to precisely control the applied rubbing load and resultant tensile stress distribution on the membrane to generate sufficient triboelectric charge (or electric potential) for site-selective deposition of Bi_2Se_3 features without introducing any mechanical damage to the nanomembrane. Figure 3 shows the OM images of two HRTEM samples after two rubbing processes using a nanostrip-cleaned rubbing template without the interfacing layer. First, under a rubbing load of 0.5 N, i.e., the typical load set for performing RISS processes on a regular silicon wafer, the nanomembrane and the support window are mechanically broken, as shown in Fig. 3(a).

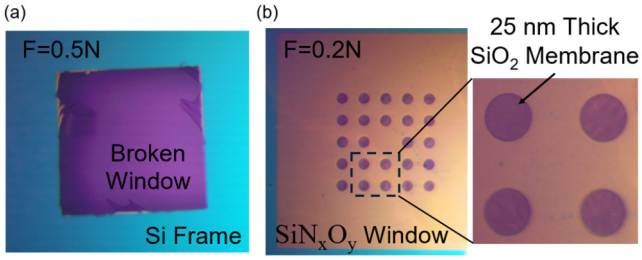

FIG. 3. OM images of the nanomembrane samples subjected to the rubbing processes using a nanostrip-cleaned rubbing template without the interfacing layer, under different loads of (a) 0.5 and (b) 0.2 N. The area marked by the dashed box is zoomed to show that no sign of Bi_2Se_3 deposition can be observed within these rubbed areas.

This clearly indicates that the resultant maximum stress on the membrane surface exceeds the tensile strength of the SiO_2 membrane. Second, under a lower load ($F = 0.2$N), no sign of Bi_2Se_3 deposition can be observed within the rubbed areas, as shown in Fig. 3(b). In this case, the vertical load is too low to generate enough triboelectric charge on the surface for enabling site-selective deposition.

To figure out the appropriate load applied on the rubbing template, quantitative analyses of the stress distribution on the nanomembrane are performed using a FEA software package included in ABAQUS tool. Figure 4(a) displays the simulation model, which consists of a single rubbing pillar and a SiO_2 nanomembrane region on a SiN_xO_y window. For calculation simplicity, we only simulate the rubbing process, in which a single rubbing pillar applies the load on a single SiO_2 sample region, and reasonably assume that by the total load is evenly distributed among

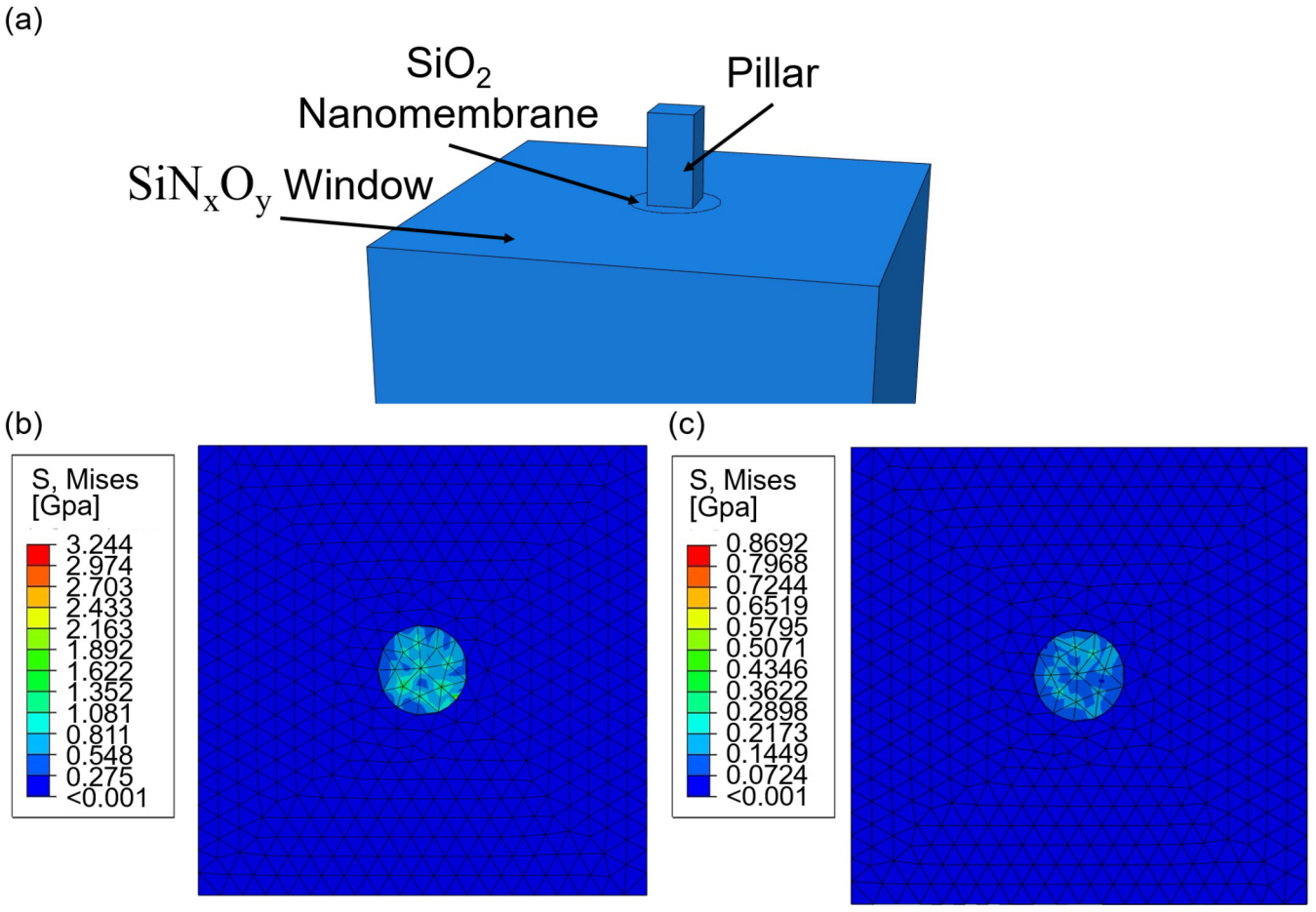

FIG. 4. FEA simulation results by an ABAQUS tool: (a) simulation model consists of a single rubbing pillar and a SiO_2 nanomembrane region on a SiNxOy window. Simulated Von Mises stress distributions over the contact area under vertical loads of (b) 0.5 and (c) 0.2 N.

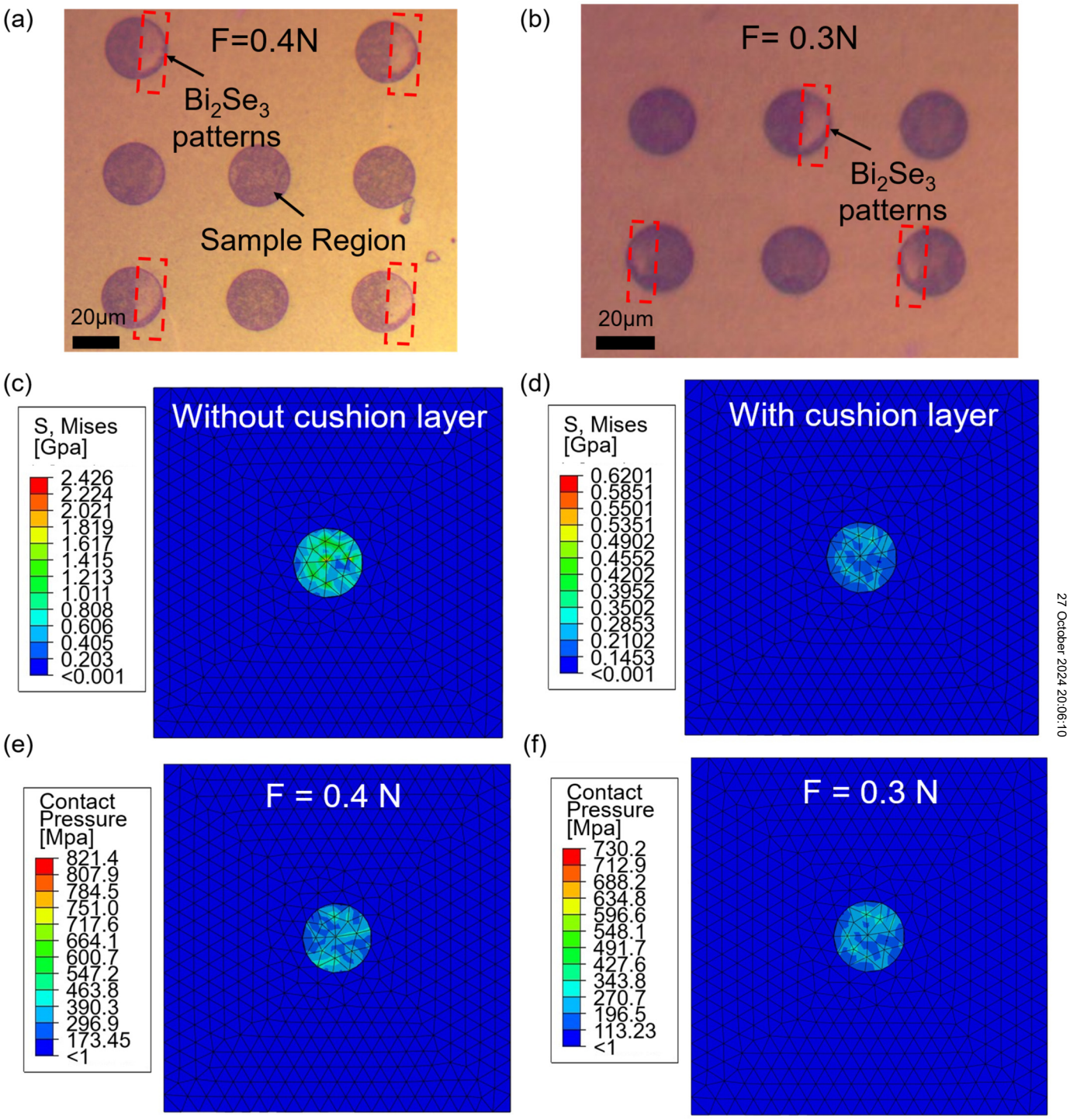

FIG. 5. OM images and FEA simulation results of the nanomembrane under different load and rubbing pillars. OM image of RISS-produced Bi_2Se_3 feature array on the nanomembranes under (a) 0.4 and (b) 0.3 N rubbing load using the rubbing template with the polymeric interfacing layer. Simulation results of the Von Mises stress distribution on the nanomembrane under 0.4 N load rubbed by (c) a cleaned rubbing pillar and (d) a pillar with an interfacing layer. Simulation result of the contact pressure distribution on the nanomembrane under applied load of (e) 0.4 and (f) 0.3 N.

24×24 pillars. Figure 4(b) shows the simulated Von Mises stress distribution over the contact area between the rubbing pillar and the membrane surface under a vertical load of 0.5 N. This result shows that such a load results in a maximum stress of 3.24 GPa within the rubbed area on the nanomembrane, which exceeds the tensile strength of SiO_2 thin films ($600 < \sigma_{ult} < 1900$ Mpa).[19] Such stress concentration on the membrane substrate is the main factor responsible for the failure of the nanomembrane. Under the load of 0.2 N, the maximum Von Mises stress on the membrane substrate decreases to 0.87 GPa, which much less likely causes the damage to the SiO_2 nanomembrane [Fig. 4(c)]. These two simulation results are consistent with the experimental rubbing results shown in Fig. 3.

In aforementioned experiments, the rubbing template is thoroughly cleaned by using the nanostrip to fully remove the remaining polymeric components. However, such relatively smooth and rigid pillar surfaces can easily generate concentrated stress when brought in contact with the SiO_2 nanomembrane surfaces. To mitigate such a stress concentration effect, as already shown in Fig. 2(b), a polymeric interfacing layer is introduced by coating the rubbing pillars with 3 μm thick photoresist followed by a brief O_2 plasma treatment. Figure 5(a) shows the OM images of the Bi_2Se_3 feature array produced on nanomembranes by using this rubbing template with the polymeric interfacing layer, under a load of 0.4 N. Here, some SiO_2 nanomembrane regions are not fully covered by Bi_2Se_3 channel features. For such a nanomembrane window, only about half of its area is rubbed by the pillar for selective deposition of Bi_2Se_3. We intentionally do this to allow the HRTEM characterization of the edge regions of RISS-produced Bi_2Se_3 channel structures. Figure 5(b) shows that under 0.3 N rubbing load, although Bi_2Se_3 nucleation occurs within the rubbed area, the resultant Bi_2Se_3 film pattern is not continuous and barely covers the whole rubbed area. This indicates that 0.3 N is a critical processing condition, and this rubbing load only generates sporadic regions with triboelectric charge density sufficient for initiating material deposition. These results indicate that 2D material patterns can be selectively formed within the rubbed areas on nanomembranes without generating any mechanical damage features.

We also perform additional FEA simulations of the RISS process using the rubbing pillars with and without polymeric interfacing layers, as shown in Figs. 5(c)–5(f). Figure 5(c) shows that a maximum Von Mises stress of 2.42 GPa appears on the nanomembrane rubbed by a cleaned rubbing pillar under 0.4 N load. For the simulation with the interfacing layer, a 3 μm thick polymeric layer is introduced on the surface of the pillars to fully cover their contact area with the substrate. Young's modulus and Poisson's ratio of the interfacing layer is 2 GPa and 0.35, respectively.[20,21] Under the same load but with the polymeric interfacing layer, the maximum Von Mises stress on the substrate decreases to 0.62 GPa [Fig. 5(d)], and the magnitude of the stress has the higher uniformity in comparison to the stress distribution in Fig. 5(c). Our previous works indicate that the areal density of rubbing-induced triboelectric charge, which can be quantitatively quantified by the resultant surface potential, is closely related to the contact pressure between the rubbing pillar and the substrate.[9,22] In our previous works, we identified that the triboelectric charge pattern with a surface potential of 100 mV serves as a benchmark threshold

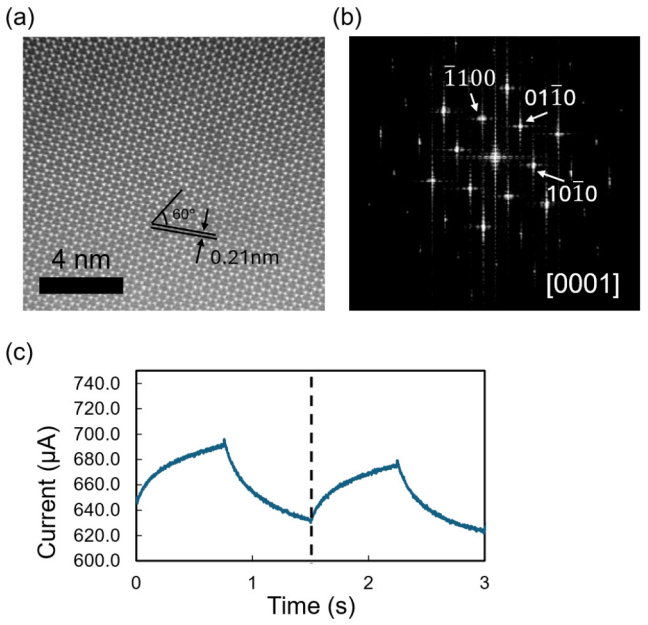

FIG. 6. RISS-produced Bi_2Se_3 features on the nanomembranes characterized by HRTEM: (a) HRTEM image of a representative RISS-produced Bi_2Se_3 feature and (b) the corresponding FFT analysis result of the HRTEM image. (c) Pulse-programmed memristive switching characteristic curve measured from a Bi_2Se_3 memristor.

condition for enabling effective site-selective growth or deposition of 2D material features, and such a condition can be generated by the rubbing process under a contact pressure of ~400 MPa on the nanomembrane.[9] Figure 5(e) displays the simulated contact pressure distribution on the nanomembrane under an applied load of 0.4 N. This simulation result shows that such a rubbing load can induce contact pressure of >400 MPa for most rubbed areas. The simulated contact pressure distribution shown in Fig. 5(e), in combination with aforementioned simulated Von Mises stress distribution in Fig. 5(d), verifies that the rubbing process under a load of 0.4 N can generate sufficiently high triboelectric charge density for enabling site-selective deposition of 2D material patterns and cause no damage to the nanomembranes. In addition, the simulation result for the contact pressure distribution under an applied load of 0.3 N [Fig. 5(f)] shows that within most rubbed areas, the contact pressure is less than 400 MPa, which is not sufficient for initiating Bi_2Se_3 nucleation. This simulation result explains the nonuniformity of the deposited Bi_2Se_3 films shown in Fig. 5(b).

The RISS-produced Bi_2Se_3 features on the nanomembranes can be directly characterized by HRTEM with no need of additional sample transfer or preparation. Figure 6(a) displays the HRTEM image of a representative RISS-produced Bi_2Se_3 feature. The HRTEM shows that RISS-deposited Bi_2Se_3 has a lattice structure with an interplanar spacing of 0.21 nm and the angle between its principal planes is 60°. Figure 6(b) shows the corresponding FFT analysis result of the HRTEM image, which further confirms that RISS-produced Bi_2Se_3 has a hexagonal single-crystal structure

with the zone axis of [0001]. Finally, a set of electrodes are deposited on RISS-produced Bi_2Se_3 channels to make lateral memristors. Figure 6(c) shows the pulse-programmed memristive switching characteristic curve measured from a representative Bi_2Se_3 memristor, which involves two consecutive programming/relaxation cycles. During the programming stage, 1000 voltage pulses with a magnitude of 5 V, duration of 1.24 ms, and duty cycle of 90% are applied to the device. For the subsequent relaxation stage, no additional pulses are applied to the device. This result demonstrates that the conductance state of a Bi_2Se_3 memristor can be repeatedly and continuously modulated to different values by application of voltage pulses and exhibit a short memory behavior. Such memristors with short-term plastic relaxation characteristics can serve as synaptic nodes for the hardware-based recurrent neural networks that need the cycle operation for processing spatiotemporal signals.[11]

IV. SUMMARY AND CONCLUSION

In summary, we demonstrate the implementation of the RISS deposition method on the SiO_2 nanomembranes and enable direct HRTEM characterization of the crystal structure of RISS-produced Bi_2Se_3 structures. The experiments show that the rubbing load of 0.5 N damages the nanomembranes, while the rubbing load of 0.2 N fails to generate enough triboelectric charge density or surface potential for initiating the site-selective deposition. Our FEA simulation results indicate that for the former case, the maximum Von Mises stress on the membrane is 3.24 GPa, which exceeds the tensile strength of the SiO_2 thin film. To avoid such a high stress concentration, a polymeric interfacing layer is coated on the rubbing pillars to serve as load cushion and distribute the stress more uniformly. With such an interfacing layer, the maximum Von Mises stress on the membrane decreases from 2.42 to 0.62 GPa under a rubbing load of 0.4 N. Furthermore, the simulation also shows that under this rubbing load, the resultant contact pressure within the rubbed area on the membrane is largely high than 400 MPa, which is sufficient to generate a triboelectric surface potential of >100 mV, capable of initiating effective site-selective deposition of 2D material features. In this work, Bi_2Se_3 patterns can be successfully deposited on the intact nanomembranes using the rubbing pillars with interfacing layers under 0.4 N load. The HRTEM image of the deposited sample shows that it has highly organized single-crystal structures. This research provides guidance for depositing 2D material patterns on nanomembranes, which could be further leveraged for other *in situ* atomic-scale material characterizations and enable new flexible electronic device fabrication routes.

ACKNOWLEDGMENTS

This work was supported by NSF Grant No. CMMI-2001036. The authors would like to thank the staff of the University of Michigan's Lurie Nanofabrication Facility for providing the support of SEM imaging, as well as Kai Sun and Michigan Center for Materials Characterization (MC^2) for HRTEM imaging.

AUTHOR DECLARATIONS

Conflict of Interest

The authors have no conflicts to disclose.

Author Contributions

Mingze Chen: Conceptualization (lead); Data curation (lead); Formal analysis (lead); Investigation (lead); Methodology (lead); Software (lead); Validation (lead); Visualization (lead); Writing – original draft (lead); Writing – review & editing (lead). **Xiaoqiu An:** Investigation (supporting); Resources (supporting). **Seungjun Ki:** Formal analysis (supporting); Investigation (supporting). **Xiaogan Liang:** Funding acquisition (lead); Project administration (lead); Resources (lead); Supervision (lead); Writing – original draft (supporting); Writing – review & editing (supporting).

DATA AVAILABILITY

The data that support the findings of this study are available from the corresponding author upon reasonable request.

REFERENCES

[1]H. Wang, H. S. Wang, C. Ma, L. Chen, C. Jiang, C. Chen, X. Xie, A.-P. Li, and X. Wang, Nat. Rev. Phys. **3**, 791 (2021).
[2]J. Wu, H. Lin, D. J. Moss, K. P. Loh, and B. Jia, Nat. Rev. Chem **7**, 162 (2023).
[3]O. Samy, S. Zeng, M. D. Birowosuto, and A. El Moutaouakil, Crystals **11**, 355 (2021).
[4]A. Taffelli, S. Dirè, A. Quaranta, and L. Pancheri, Sensors **21**, 2758 (2021).
[5]U. Sundararaju, M. A. S. Mohammad Haniff, P. J. Ker, and P. S. Menon, Materials **14**, 1672 (2021).
[6]S. Moon, J. Kim, J. Park, S. Im, J. Kim, I. Hwang, and J. K. Kim, Adv. Mater. **35**, 2204161 (2023).
[7]Y. S. Na *et al.*, 2D Mater. **8**, 045041 (2021).
[8]Q. Ma, G. Ren, K. Xu, and J. Z. Ou, Adv. Opt. Mater. **9**, 2001313 (2021).
[9]B. Ryu, D. Li, C. Park, H. Rokni, W. Lu, and X. Liang, ACS Appl. Mater. Interfaces **10**, 43774 (2018).
[10]M. Chen, S. Ki, and X. Liang, J. Vac. Sci. Technol. B **39**, 062203 (2021).
[11]M. Chen, S. J. Ki, and X. Liang, ACS Appl. Electron. Mater. **5**, 3830 (2023).
[12]S. Ki, M. Chen, and X. Liang, J. Vac. Sci. Technol. B **39**, 062201 (2021).
[13]S. Ki, M. Chen, and X. Liang, IEEE Nanotechnol. Mag. **17**, 24 (2023).
[14]S. J. Ki, J. Kim, M. Chen, and X. Liang, Appl. Phys. Lett. **123**, 223501 (2023).
[15]A. Mukundan, Y.-M. Tsao, S. B. Artemkina, V. E. Fedorov, and H.-C. Wang, Nanomaterials **12**, 135 (2022).
[16]F. Lyu, B. Tang, X. Li, and Q. Chen, Nanotechnology **33**, 345702 (2022).
[17]Z. L. Wang and A. C. Wang, Mater. Today **30**, 34 (2019).
[18]D. Liu *et al.*, Nat. Commun. **13**, 6019 (2022).
[19]W. Sharpe, J. Pulskamp, D. Gianola, C. Eberl, R. Polcawich, and R. Thompson, Exp. Mech. **47**, 649 (2007).
[20]R. H. Alasfar, S. Ahzi, N. Barth, V. Kochkodan, M. Khraisheh, and M. Koç, Polymers **14**, 360 (2022).
[21]O. Olabisi, in *Handbook of Thermoplastics*, edited by O. Olabisi and K. Adewale (CRC, Boca Raton, 2016), pp. 1–2.
[22]M.-L. Seol, S.-H. Lee, J.-W. Han, D. Kim, G.-H. Cho, and Y.-K. Choi, Nano Energy **17**, 63 (2015).